Single-image wavefront curvature sensing

Paul Hickson and Greg Burley

University of British Columbia, Department of Geophysics and Astronomy
2219 Main Mall, Vancouver, British Columbia V6T 1Z4, Canada

ABSTRACT

A single defocussed star image contains sufficient information to uniquely determine the spatial phase fluctuations of the incident wavefront. A sensor which responds to the intensity distribution in the image produces signals proportional to the wavefront curvature within the pupil and the radial slope at the pupil boundary. Unlike Roddier's differential curvature sensing technique, a single-image sensor does not cancel intensity fluctuations due to atmospheric scintillation. However, it has been shown that at typical astronomical sites the scintillation signal is negligibly small. A single-image curvature sensor can theoretically achieve a signal-to-noise ratio of order $\mathcal{Q} \simeq r_0^2/\lambda z_0$ where r_0 is Fried's correlation length, λ is the wavelength, and z_0 is the root-mean-square distance through the atmosphere, weighted by the refractive index structure constant C_n^2. This is more than adequate for AO systems whenever $D/r_0 \lesssim \mathcal{Q}^{6/5}$. Such a sensor can be very simple, optically and mechanically, and has lower detector read noise than a comparable differential system. The concept has been tested in the laboratory by introducing, and detecting, spherical aberration in a simple optical system.

1. INTRODUCTION

In recent years, advances in adaptive optics (AO) systems have offered the prospect of providing large ground-based astronomical telescopes with near-diffraction limited performance over a wide range of wavelengths. A key component of all AO systems is a wavefront sensor which measures residual phase distortion, due to atmospheric turbulence, in the wavefront of light received from a reference star. This information is then used to drive an electromechanical flexible mirror which corrects the wavefront providing sharper images for all objects in the vicinity of the star.

F. Roddier and collaborators[1,2,3] have developed an elegant wavefront sensor which uses the difference between two out-of-focus star images, one before the focus and one after, to directly measure the curvature of the wavefront, and its radial slope. This technique has many advantages, not the least of which is that it provides a natural interface to membrane and piezoelectric bimorph mirrors in which electrical signals induce curvature directly. This alleviates the need for complex real-time calculations.

While the Roddier technique is relatively simple and effective, it does require the near-simultaneous (at least within a few ms) measurement of two separate images, at equal distances before and after the focus. This requires a beam splitter and either two separate detectors or a vibrating mirror to direct both images onto a single detector. In either case, since the difference of the intensities is required, the noise resulting from detector readout is increased by a factor of $\sqrt{2}$ over that derived from a single image.

This paper describes a simpler system in which the curvature signal is derived from the fluctuating component of the intensity in a single image. We show that for practical astronomical AO systems, such a sensor can theoretically perform at least as well as a differential system. A more detailed analysis of the theoretical performance of the single-image curvature sensor has been presented elsewhere[4]; in this paper we summarize the main results of that study, and describe preliminary results of laboratory tests of a single-image curvature sensor.

2. CURVATURE SENSING

Roddier[1] has shown that in the geometrical approximation, phase fluctuations in a wavefront incident on a lens

0-8194-1496-4/94/$6.00

or mirror lead to intensity fluctuations in a defocussed image in proportion to the wavefront curvature. For a ray passing through position $\mathbf{r}$ in the entrance pupil (assumed to be coincident with the mirror or lens), the intensity fluctuation measured at a distance s from the pupil is given by[4]

$$\frac{\Delta I}{I_0}(\mathbf{r}) = -\frac{s}{k\beta}\left[\nabla^2\phi(\mathbf{r}) - \delta(r-R)\frac{\partial\phi(\mathbf{r}))}{\partial r}\right], \tag{1}$$

where ϕ is the wavefront phase,

$$\beta = (f-s)/f \tag{2}$$

is the demagnification factor, f and R are the focal length and radius of the mirror, $k = 2\pi/\lambda$ is the wave number and I_0 is the non-fluctuating part of the intensity. The delta function $\delta(r-R)$ represents a linear impulse distribution around the edge of the pupil, and r is the length of the vector $\mathbf{r}$. The wavefront phase is defined here in the same sense as Hamilton's point characteristic function Φ of the optical system[5], which is a measure of the optical path length. Specifically, we adopt $\phi = k\Phi$.

In obtaining Eq. (1), the condition

$$\frac{\lambda s}{\beta} << r_0^2 << R^2 \tag{3}$$

was assumed to hold, where r_0 is the correlation scale of the fluctuations[6]. The lower limit ensures that the diffraction pattern arising from the scale r_0 is small compared to the image scale βr_0. Eq. (1) differs slightly from the equation derived by Roddier, and does not require that $\beta << 1$.

In addition to the fluctuation in intensity due to curvature of the incident wavefront, there will also be a contribution to ΔI from spatial variations in the amplitude of the incident radiation (scintillation). Roddier's technique combines intensities measured simultaneously at two locations, a small distance Δs before and after the geometric focus, in order to cancel such amplitude fluctuations: for images located at $s = f \pm \Delta s$ the coefficients β have equal magnitude but opposite sign so the intensity fluctuations due to curvature are very nearly equal, but opposite. The component of ΔI that is due to scintillation increases with distance from the turbulent layers, but for astronomical applications this distance is of the order of several km, much larger than Δs, so the scintillation components are practically identical at the two image positions, and have the same sign. By taking the difference between the two images, the scintillation components almost completely cancel, whereas the curvature components add.

3. A SINGLE-IMAGE CURVATURE SENSOR

From Eq. (1) it is clear that the wavefront curvature information is present in a single defocussed image. This curvature information can be extracted from the difference of the local intensity $I(\mathbf{r})$ and a constant signal I_0. In essence, one compares the intensity in the defocussed image with that of a "model" image which can be stored, for example, in computer memory. In a practical wavefront sensor, the pupil is divided into a finite number of subapertures within which the local intensity is integrated. For a single-image sensor, one would simply take the difference, for each subaperture, between the instantaneous signal and suitable constants. These constants are the signals expected, from each supaperture, for a circular image of uniform intensity. They can be obtained either from a temporal average of the signals from each subaperture, or by dividing the total signal by the effective fractional geometrical area of the subaperture. Variations in wavefront tilt, represented by the delta function in Eq. (1), as well as defocus, result in difference signals in subapertures located at the edge of the pupil.

Because it uses information from only one side of the focus, a single-image sensor cannot cancel scintillation noise as does a differential sensor. Clearly, a single-image sensor can only be practical if the response of a detector to fluctuations due to scintillation is small compared to its response to wavefront curvature fluctuations. Hickson[4] has shown that scintillation effects are indeed small for typical astronomical applications. The relative strength of curvature

and scintillation effects on the signal produced by the wavefront sensor can be described by the dimensionless ratio

$$\mathcal{Q} = \frac{< \Delta S_C^2 >^{1/2}}{< \Delta S_A^2 >^{1/2}} , \tag{4}$$

which is the ratio of variances of the signal produced by curvature and amplitude fluctuations. The angular brackets denote an ensemble average. For a Kolmogorov turbulence spectrum, it is shown[4] that

$$\mathcal{Q} \simeq \frac{s}{\beta z_0} , \tag{5}$$

where z_0 is the C_n^2-weighted RMS line of sight distance through the atmospheric turbulence, and C_n is the refractive index structure constant.

The curvature sensor is most efficient when the size of a subaperture is matched to the atmospheric seeing. This condition is

$$\frac{\lambda s}{r_0} = \beta a , \tag{6}$$

where $2a$ is the typical linear dimension of the region, in the entrance pupil, which is imaged onto the subaperture. This gives

$$\mathcal{Q} = \frac{r_0 a}{\lambda z_0} . \tag{7}$$

For astronomical applications, a will be at least as large as r_0, which is typically $0.3\text{m}(\lambda/0.5\text{um})^{6/5}$ at the best astronomical sites[7,8]. An additional restriction comes from the C_n^2 term. Observations from Mauna Kea[7] indicate that $z_0 \simeq 4$ km. Thus we have

$$\mathcal{Q} \gtrsim 45(\lambda/0.5\text{um})^{7/5} , \tag{8}$$

which shows that the scintillation noise is typically less than about 2% of the curvature signal. It's effect will generally be negligible in comparison to photon noise.

While the above analysis refers to measurements of wavefront curvature, is can also be shown[4] that a similar result holds for the subapertures which measure the radial slope of the wavefront. The signal from these subapertures is typically larger than those from the curvature-sensing subapertures, while the scintillation noise is somewhat smaller. As a result, scintillation provides an even smaller contribution to the total noise.

4. APPLICATIONS

Single image curvature sensors have potential applications in many areas. For active optics (aO) applications, high-spatial-frequency phase information can be obtained by projecting a defocussed star image onto a CCD detector. For integration times exceeding several minutes, atmospheric fluctuations effectively average to zero. Phase errors introduced by the optical system can then be estimated from the intensity distribution in the image. For example, a modal expansion can be made of the wavefront phase, and the expansion coefficients determined by least-squares analysis of the measured intensities[9].

A related application is for fast guiding of large telescopes. A small CCD can be attached to a guide probe (or illuminated by associated relay optics). This CCD can have a sufficient field of view to locate and acquire guide stars when positioned in the focal plane. By defocussing the image, either by moving the CCD or a relay lens, the CCD becomes a single image curvature sensor. The subaperture geometries are then determined by software. On-chip binning can be used to reduce read-noise. Such a sensor can provide information not only on wavefront slope (tracking error), but also defocus, astigmatism, and higher-order aberrations if desired.

A final application that we will consider is in adaptive optics (AO). In AO systems, high quantum efficiency and low noise are of paramount importance in a wavefront sensor. With no reimaging, beamsplitting, or relay optics, single-image curvature sensors employing high-quantum-efficiency CCD detectors, offer the prospect of very high efficiency. As noted, the detector read noise associated with the measurement is smaller by a factor of $\sqrt{2}$ than that of a differential system.

In typical AO systems, the signal-to-noise ratio is limited by photon noise because bright guide stars are rarely sufficiently close to the object of interest. In this case a single-image sensor should perform at least as well as a differential system. For high signal-to-noise ratio applications, a single-image sensor will ultimately be limited by scintillation noise. In that case, one can show[4] that the structure function $\mathcal{D}^{AO}$ of the AO corrected wavefront has the form

$$\mathcal{D}^{AO}(r) \simeq \mathcal{Q}^{-2} 2\mathcal{D}(r) \tag{9}$$

where D is the structure function of the uncorrected wavefront. (The structure function described here is the sum of the mean square phase and intensity differences between two points on the wavefront separated by a distance r). For Kolmogorov turbulence, D has the form

$$\mathcal{D}(r) = 6.88(r/r_0)^{5/3} \, . \tag{10}$$

From this we see that an AO system employing a single-image curvature sensor can theoretically increase the effective correlation length r_0 by a factor $\mathcal{Q}^{6/5}$. At good astronomical sites this corresponds to a scale which exceeds the diameters of the largest optical telescopes, indicating that scintillation noise will not be a limiting factor in AO applications of single-image curvature sensors.

5. LABORATORY TESTS

With a simple optical system involving a short focal length lens and a pinhole illuminated by a light-emitting diode, we have recorded some single beyond-focus images on a small 64 × 64 CCD. The pinhole and CCD were centred on the optical axis of the lens. This arrangement allowed us to measure the primary spherical aberration of the system, which has the form

$$\phi(r) = -\frac{kB}{4R^4} r^4 \tag{11}$$

where B is the Seidel coefficient of spherical aberration. Substituting this expression in Eq. (1), gives

$$\frac{\Delta I}{I_0} = \frac{4sB}{\beta R^4} r^2 \, , \tag{12}$$

i.e. , the intensity fluctuation has a quadratic dependence on radius in the pupil.

A series of images were produced from a 5 ms exposures followed by the usual CCD bias removal and flat fielding process. After computing the mean intensity I_0 over the aperture, the curvature map was extracted from $I(r)$ and I_0 on a pixel by pixel basis.

Figure 1 shows a cross-section through the center of one of the processed curvature maps. The smooth curve is the best least-squares parabolic fit to the data. It has the form $\Delta I/I_0 \simeq -0.6(r/R)^2$. For the experimental setup used, $f = 70$ mm, $s = 72.8$ mm, $R = 13.75$ mm, and $\beta = -0.040$. Eq. (12) then gives $B = 0.0156$ mm which corresponds to 5.7 waves of spherical aberration

6. ACKNOWLEDGEMENTS

We are pleased to acknowledge financial support from the Natural Sciences and Engineering Research Council of Canada.

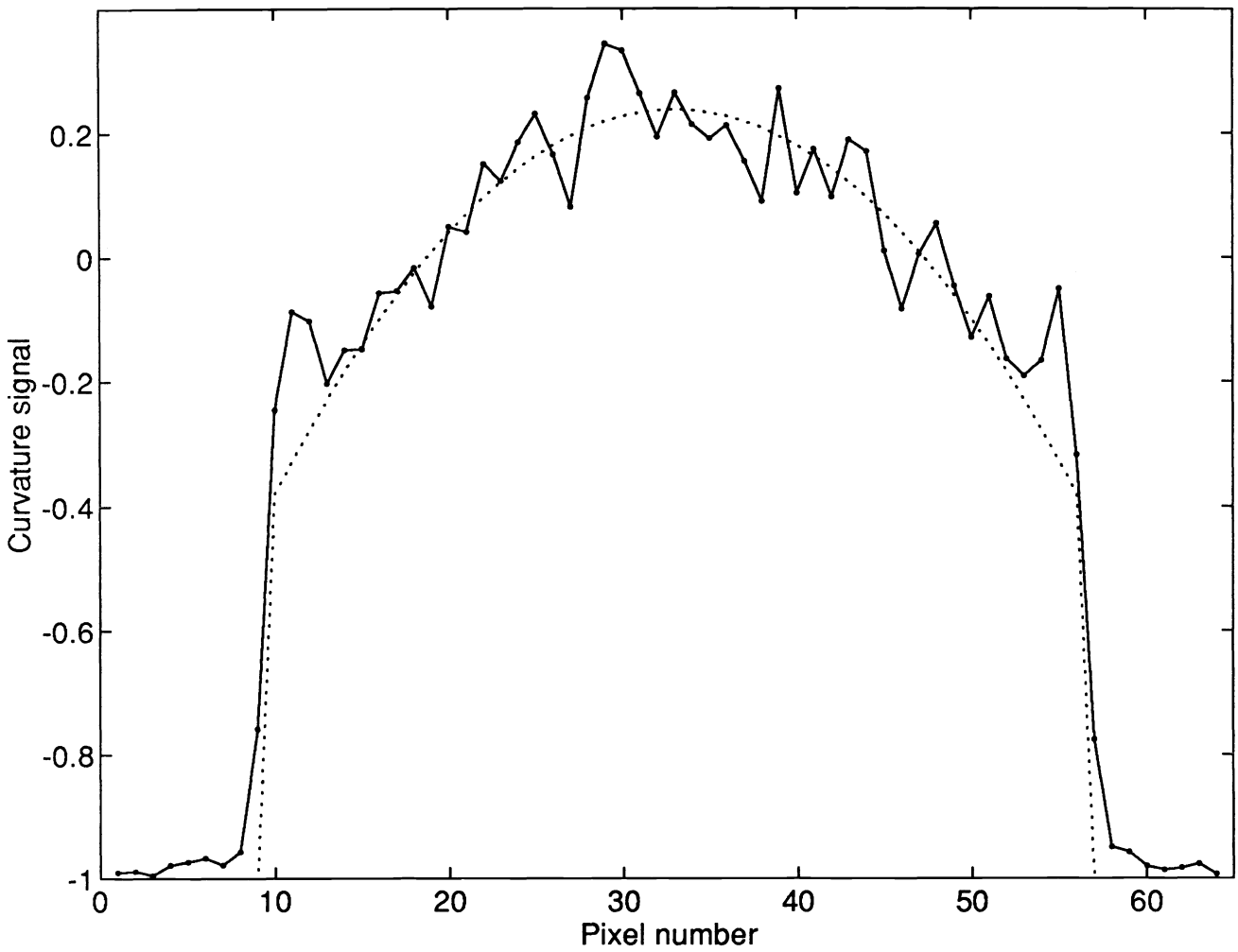

Figure 1. Sample cross-section of a 64x64 curvature map with a parabolic fit to the $\Delta I/I_0$ curvature signal showing 5.7 waves of spherical aberration.

7. REFERENCES

1. F. Roddier, "Curvature sensing: a diffraction theory," *NOAO R&D Note* 87-3 (1987).
2. F. Roddier, "A new concept in adaptive optics: curvature sensing and compensation," *Appl. Optics* 27, 1223-1225 (1988).
3. F. Roddier, C. Roddier and N. Roddier, "Curvature sensing: a new wavefront sensing method," *Proc. Soc. Photo-Opt. Instrum. Eng.* 976, 203-209 (1988).
4. P. Hickson, "Wavefront Curvature Sensing from a Single Defocussed Image," *J. Opt. Soc. Am.*, in press (1994).
5. M. Borne and E. Wolf, *Principles of Optics*, 6th ed. (Pergamon Press Ltd., Oxford, 1980).

6. D. L. Fried, "Optical resolution through a randomly inhomogeneous medium for very long and very short exposures," *J. Opt. Soc. Am.* 56, 1372-1379 (1966).

7. F. Roddier, L. Cowie, J. E. Graves, A. Songaila, D. McKenna, J. Vernin, M. Azouit, J. L. Caccia, E. Limburg, C. Roddier, D. Salmon, S. Beland, D. Cowley, and S. Hill, "Seeing at Mauna Kea: a joint UH-UN-NOAO-CFHT study," in *Advanced Technology Optical Telescopes IV*, L. D. Barr, ed., *Proc. Soc. Photo-Opt. Instrum. Eng.* 1236, 485-491 (1990).

8. B. L. Ellerbroek, "Adaptive optics performance predictions for large telescopes under good seeing conditions," in ESO Conf. on *Progress in Telescope and Instrumentation Technologies*, M.-H. Ulrich, ed., 411-413 (1992).

9. P. Hickson, "Modal estimation of wavefront phase by means of curvature sensing," in preparation (1994).